Carbohydrate Polymers 111 (2014) 530–537

Contents lists available at ScienceDirect

Carbohydrate Polymers

journal homepage: www.elsevier.com/locate/carbpol

Electrospun chitosan nanofibers with controlled levels of silver nanoparticles. Preparation, characterization and antibacterial activity

Sang Jin Lee[a,b,1], Dong Nyoung Heo[a,1], Ji-Hoi Moon[a], Wan-Kyu Ko[a], Jung Bok Lee[a], Min Soo Bae[a], Se Woong Park[a], Ji Eun Kim[a], Dong Hyun Lee[a,b], Eun-Cheol Kim[c], Chang Hoon Lee[d], Il Keun Kwon[a,*]

[a] Department of Maxillofacial Biomedical Engineering and Institute of Oral Biology, School of Dentistry, Kyung Hee University, 26 Kyunghee-daero, Dongdaemun-gu, Seoul 130-701, Republic of Korea
[b] Department of Dentistry, Graduate School, Kyung Hee University, 26 Kyunghee-daero, Dongdaemun-gu, Seoul 130-701, Republic of Korea
[c] Department of Maxillofacial Tissue Regeneration, School of Dentistry and Research Center for Tooth and Periodontal Regeneration (MRC), Kyung Hee University, 26 Kyunghee-daero, Dongdaemun-gu, Seoul 130-701, Republic of Korea
[d] Department of Oriental Gynecology, College of Oriental Medicine, Kyung Hee University, 26 Kyunghee-daero, Dongdaemun-gu, Seoul 130-701, Republic of Korea

ARTICLE INFO

Article history:
Received 16 August 2013
Received in revised form 1 April 2014
Accepted 8 April 2014
Available online 20 April 2014

Keywords:
Silver nanoparticle
Chitosan
Nanofiber
Electrospinning
Antibacterial effect

ABSTRACT

The ideal wound dressing would have properties that allow for absorption of exudates, and inhibition of microorganism for wound protection. In this study, we utilized an electrospinning (ELSP) technique to design a novel wound dressing. Chitosan (CTS) nanofibers containing various ratios of silver nanoparticles (AgNPs) were obtained. AgNPs were generated directly in the CTS solution by using a chemical reduction method. The formation and presence of AgNPs in the CTS/AgNPs composite was confirmed by x-ray diffraction (XRD), ultraviolet-visible spectroscopy (UV) and thermogravimetric analysis (TGA). The electrospun CTS/AgNPs nanofibers were characterized morphologically by scanning electron microscopy (SEM) and transmission electron microscopy (TEM). These nanofibers were subsequently tested to evaluate their antibacterial activity against gram-negative *Pseudomonas aeruginosa* (*P. aeruginosa*) and gram-positive Methicillin-resistant *Staphylococcus aureus* (MRSA). Results of this antibacterial testing suggest that CTS/AgNPs nanofibers may be effective in topical antibacterial treatment in wound care.

1. Introduction

Since the 1930s, electrospinning (ELSP) has been applied to generate diverse nanofibrous textiles for various applications such as filters, skin masks, semipermeable membrane, clothing, and medical materials (Burger, Hsiao, & Chu, 2006; Greiner & Wendorff, 2007). Recently, nanofibers have been applied towards medical uses such as drug delivery systems, tissue engineering scaffolds, vascular grafts, biological wound dressings, and support for the human body (Pham, Sharma, & Mikos, 2006; Xie, Li, & Xia, 2008; Yoshimoto, Shin, Terai, & Vacanti, 2003). These nanofibers have found a wide array of uses due to their high surface area resulting from the nano-to-micro sized fibers and high porosity. Additionally, nanofibers have a high capacity for loading of biological substances and active materials such as gold or silver nanoparticles (Jin et al., 2013; Rujitanaroj, Pimpha, & Supaphol, 2008).

For several years, chitosan (CTS) has been widely studied for use in the biomedical industry. For example, it has been used as a biological adaptation material, drug delivery vehicle, bone tissue scaffold, and as wound dressings (Bhattarai et al., 2009; Khor & Lim, 2003). CTS is the second most abundant polysaccharide on earth and is a copolymer comprised of glucosamine and acetylglucosamine units linked by –(1,4) glucosidic bonds (Guibal, 2005; Lee, Jeong, Kang, Lee, & Park, 2009). This is an attractive natural polymer for biomedical use due to its reported biocompatibility and biodegradability, as well as its reported desirable bioactive properties such as anti-microbial activity, scar reduction and wound healing (Bhardwaj & Kundu, 2010; Elsabee, Naguib, & Morsi, 2012; Mahoney, Mccullough, Sankar, & Bhattarai, 2012; Muzzarelli & Muzzaralli, 2005). CTS can be readily prepared as porous nanofibers by electrospinning (Jayakumar, Prabaharan, Nair, & Tamura, 2010; Sencadas et al., 2012).

Contamination of wounds by bacteria is a common problem, prevention of wound contamination is important and an efficacious

* Corresponding author. Tel.: +82 2 961 0350.
E-mail address: kwoni@khu.ac.kr (I.K. Kwon).
[1] These authors equally contributed to this work.

http://dx.doi.org/10.1016/j.carbpol.2014.04.026
0144-8617/

antimicrobial dressing may help to promote normal wound healing. AgNPs have demonstrated enhanced antibacterial efficacy in vitro (Morones et al., 2005) and may prove to be good candidates for topical antibacterial wound care (Atiyeh, Costagliola, Hayek, & Dibo, 2007; Storm-Versloot, Vos, Ubbink, & Vermeulen, 2010). Additionally, AgNPs can be easily synthesized using silver nitrate reduced by sodium borohydride (Shameli et al., 2011). When CTS and silver are mixed silver nitrate is chelated by the CTS (Reicha, Sarhan, Hamid, & Sherbiny, 2012). In terms of antibacterial effectiveness, AgNPs can be easily applied to a variety of medical devices such as dental materials (Rai et al., 2009), catheters (Chaloupka, Malam, & Seifalian, 2010), coating of biomaterials (Pal, Tak, & Song, 2007), and burn wound dressings (Lago, Oliveira, Gonçalves, Kobarg, & Cardoso, 2011).

Recently, many types of AgNPs have been loaded into a variety of nanofibrous scaffolds for antimicrobial applications. These include PHBV (Xing et al., 2010), PMMA (Kong & Jang, 2008a,b), PTBAM (Song, Kang, Lee, Hwang, & Jang, 2012), PVP (Jin, Lee, Jeong, Park, & Youk, 2005), Polyrhodanine (Kong & Jang, 2008a,b), and blends of materials such as CTS/PVA (Hang, Tae, & Park, 2010), CTS/PEO (Fouda, El-Aassar, & Al-Deyab, 2013), CTS/Gelatin (Zhuang, Cheng, Kang, & Xu, 2010). In terms of blending of CTS with silver nanocomposites or films, these have previously been reported to possess excellent antimicrobial activity (López-Carballo, Higueras, Gavara, & Hernández-Muñoz, 2013; Twu et al., 2008). In the previous study (Cao, Cheng, Ma, & Zhao, 2010), CTS/AgNPs composites displayed a higher activity against bacteria than the use of CTS composites alone. Until recently, CTS/AgNPs nanofiber research was conducted by blending with other polymers and different kinds of CTS/AgNPs morphology. For the current research, we performed chemical reduction and ELSP to form CTS/AgNPs nanofibers without any additional blended polymer materials.

The objective of this study is to prepare and characterize controlled loadings of nanoparticluate silver in chitosan nanofibers with further investigation of their antibacterial efficacy in a zone of inhibition antibacterial test system. That is to generate pure CTS nanofibers loaded with the AgNPs by ELSP technique. The physicochemical properties of these scaffolds were analyzed by ultraviolet–visible absorption spectra (UV), transmission electron microscopy (TEM), scanning electron microscopy (SEM), thermo gravimetric analysis (TGA), and X-ray diffraction (XRD). To evaluate the antibacterial effectiveness of CTS/AgNPs nanofibers, we prepared CTS/AgNPs nanofibers with varying quantities of AgNPs as the inhibition of various bacteria may be dose dependent. *Pseudomonas aeruginosa* (*P. aeruginosa*) and Methicillin-resistant *Staphylococcus aureus* (MRSA) have been previously reported to be potent skin tissue bacteria (Rujitanaroj et al., 2008; Fouda et al., 2013; Shameli et al., 2011). Thus, we choose these bacteria for our wound dressing experiment. Testing was performed *in vitro* to determine the activity of the CTS/AgNPs against *P. aeruginosa* and MRSA.

2. Experimental: materials and methods

2.1. Materials

Chitosan powder (average MW, 370 kDa; deacetylation degree, 85%), silver nitrate (ACS reagent, ≥99.0%), and trifluoroacetic acid (ReagentPlus®, 99%) were purchased from Sigma–Aldrich (St. Louis, MO). Dichloromethane (Extra Pure, 99.0%$^{+}$) was purchased from Junsei (Junsei Chemical Co. Ltd, Japan). Sodium borohydride ($NaBH_4$) was purchased from TCI (Tokyo Chemical Industry CO., Ltd., Japan). Sodium Hydroxide (NaOH) was purchased from YPC (Yakuri Pure Chemicals CO., Ltd. Japan). Methyl alcohol (MeOH) was purchased from DaeJung (Chemical & Metals Co. Ltd., Korea). Deionized-distilled water (DDW) was produced by an ultrapure water system (Puris-Ro800; Bio Lab Tech., Korea). The membrane tube, for CTS/AgNPs composite dialysis, was purchased from Spectrum Spectra (Spectra/Por 4 dialysis tubing, 12–14 K MWCO, 45 mm flat width, 100-ft length). *P. aeruginosa* ATCC 27853 and Methicillin-resistant *S. aureus* ATCC 700787 were obtained from the American Type Culture Collection (Manassas, VA). All other reagents and solvents were of analytical grade and used without further purification.

2.2. Preparation of CTS/AgNPs composite

Initially, 4.0 g of CTS was dissolved in 200 ml of 1% acetic acid to form a 2 wt.% solution at 4 °C. After complete dissolution of CTS, the solution was stored at room temperature for 24 h. This solution at room temperature was then vacuum filtered to remove impurities using filter paper (around 10 μm). To this solution 200 ml of 10 mM silver nitrate in DDW was added with stirring for 2 h. This was performed with protection from light in order to prevent any change of the suspension color. In order to synthesize AgNPs within the chitosan solution, 80 ml of 40 mM sodium borohydride in DDW was added to the CTS solution containing silver nitrate and stirred for 1 h. In order to obtain the CTS/AgNPs composite, CTS/AgNPs solution was then poured into a 1 N NaOH in 100 ml of DDW solution. As a result, CTS/AgNPs solution solidified. The synthesized CTS/AgNPs composite was then rinsed with DDW until it reached a pH 7 and then dialyzed and freeze-dried.

2.3. Fabrication of CTS/AgNPs nanofiber via ELSP

The nanofibers were fabricated via ELSP using a 5 wt.% CTS and CTS/AgNPs solutions at mixing ratios of 100:0, 0:100, 50:50, 67:33, 83:17 (AgNPs contents = 0, 0.7, 1.3, 2, and 4 wt.% of CTS), respectively. ELSP was carried out according to the following conditions. Briefly, CTS/AgNPs composite was dissolved in a mixed TFA/DCM (7:3) solvent to produce a 5 wt.% solution. For ELSP, the polymer solution was loaded into a luer-lock syringe attached to a metal blunt needle (22 G, Kovax-needle, Korea Vaccine Co., Ltd., Korea) and electrospun on an aluminum foil covered rotating mandrel at 23 kV using a high-voltage DC power supply (Nano NC, Korea) with a 1 ml/h feed rate (KDS-200, KD Scientific Inc.) and a 15 cm needle tip-to-collector distance. The resultant CTS/AgNPs nanofiber was dried overnight under vacuum in order to remove any residual solvent. For neutralization, the dried CTS/AgNPs nanofibers were immersed in 50 ml of 3.2 M NaOH/MeOH (neutralization solution) for ten minutes, follow by rinsing with DDW until the pH reached 7. After this the CTS/AgNPs nanofibers were freeze-dried.

2.4. Ultraviolet–visible spectroscopy (UV)

In order to confirm the presence of AgNPs in the CTS/AgNPs solution, ultraviolet–visible spectrophotometry was performed using an UV1650PC (Shimadzu, Japan). The ultraviolet–visible spectrum was measured over the wavelength range of 300–700 nm. The CTS solution containing silver nitrate (10 mM) was used as the reference blank. This was compared against another specimen which was filled with the CTS solution containing sodium borohydride (40 mM) reduced silver nitrate (10 mM) diluted fivefold at room temperature.

2.5. X-ray diffraction (XRD)

To confirm the crystalline structure of the AgNPs in the CTS/AgNPs composite, XRD patterns were recorded with both dry CTS and CTS/AgNPs nanocomposites respectively using an X'pert PRO (PANalytical, USA) at a voltage of 45 kV and a current of 20 mA

with Cu Kα (λ = 0.154 nm) radiation in a 2θ range from 10° to 70°. The measurement was repeated three times.

2.6. Thermogravimetric analysis (TGA)

In order to characterize the thermal decomposition profiles of both CTS and CTS/AgNPs composites, TGA was performed on a TGA-50 (Shimadzu, Japan). Dry, 5 mg, specimens of either CTS or CTS/AgNPs composites were measured with a nitrogen flow rate of 50 ml/min and at a heating rate of 10 °C min^{-1} in a temperature range from 25 °C to 800 °C. The measurement was repeated three times.

2.7. Viscometry (viscometer)

To investigate a viscosity of ELSP solution, the solution was measured by sine-wave Vibro Viscometer (SV-10, A&D Company, Ltd., Japan) with a range from 0.3 mPa s to 10,000 mPa s with a vibration frequency of 30 Hz. All measurements were carried out at room temperature. The solution samples were prepared by following conditions. Briefly, CTS and CTS/AgNPs (AgNPs contents of 0, 4, 2, 1.3 and 0.7 wt.%) composites were dissolved in a mixed TFA/DCM (7:3) solvent to produce a 5 wt.% solution. The measurement was repeated three times.

2.8. Transmission electron microscopy (TEM)

To verify the presence and quantity of AgNPs in the CTS/AgNPs nanofibers, TEM observations were carried out using a TEM by H-7100 (Hitachi, Japan) at an accelerating voltage of 100 kV at room temperature. Specimens of CTS nanofiber alone or various ratios of CTS/AgNPs nanofibers were applied to a 200 mesh copper grid (grid hole size; 97um) coated with Formvar/carbon (Catalog No. 01801, Ted Pella Inc., USA) and dried at room temperature prior to imaging.

2.9. Scanning electron microscopy (SEM)

The surface morphologies of CTS nanofibers and CTS/AgNPs nanofibers were carried out using a scanning electron microscope (SEM, Hitachi S-2300, Japan) at acceleration voltage of 15 kV. All samples were dried at room temperature, and then sputter-coated with gold by an IB-3 (Eiko, Japan) for 10 min. The matrix morphology and fibrous diameter characterization were carried out using image analysis software (Eyeview-Analyzer (Digiplus, Korea)).

2.10. Zone of inhibition testing of antibacterial efficacy. P. aeruginosa and MRSA

P. aeruginosa ATCC 27853 and MRSA ATCC 700787 were obtained from the American Type Culture Collection (Manassas, VA). They were grown aerobically in Mueller-Hinton broth (Difco Laboratories, Detroit, MI) at 35 °C for 18 h. Disc diffusion tests were carried out according to the guidelines of the Clinical and Laboratory Standards Institute (CLSI, 2006) using Mueller-Hinton Agar (Difco). Briefly, the agar surface was inoculated by using a swab dipped in the bacterial cell suspension adjusted to a turbidity of 0.5 McFarland standard units and then allowed to dry for approximately 5 min. After placement of CTS containing discs (8 mm), the susceptibility plates were incubated at 35 °C for 16–18 h. Inhibition zones around the discs were measured in millimeters (mm) using a ruler.

3. Results and discussion

3.1. Characterization of the synthesized CTS/AgNPs solution (UV, TEM)

CTS/AgNPs solution was obtained by the reduction of silver nitrate using sodium borohydride in CTS solution. In the first step, silver nitrate was added to the CTS solution. The silver ions within

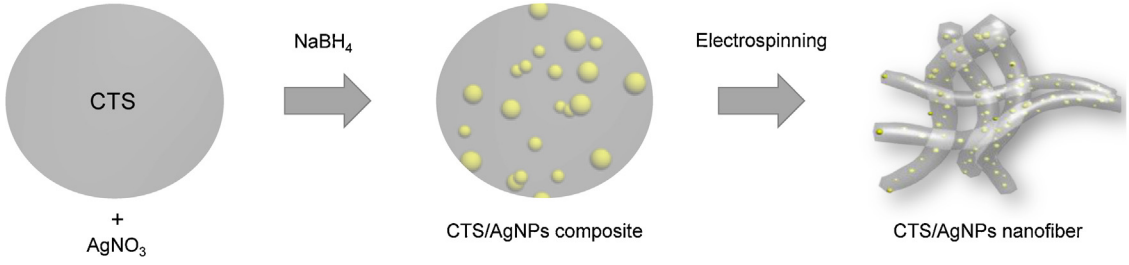

Fig. 1. Schematic diagram of CTS/AgNPs nanofiber generation.

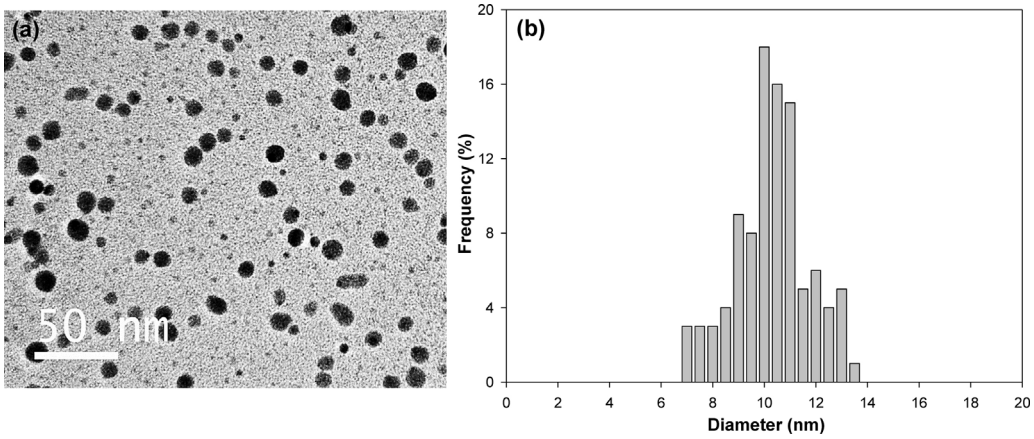

Fig. 2. TEM image of AgNPs in composite solution (a), size distribution of AgNPs in composite (b).

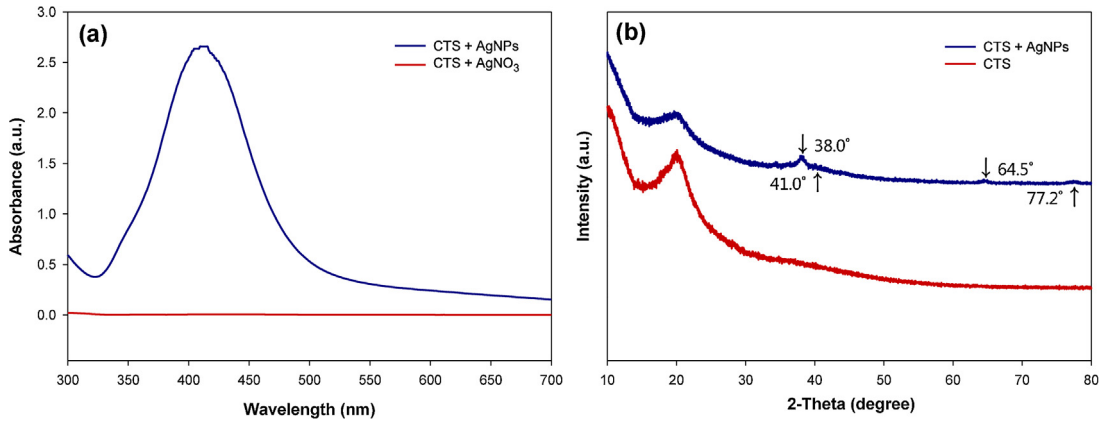

Fig. 3. UV–vis spectra of AgNPs reduced with NaBH4 in AgNO3 embedded CTS solution (a). NaBH4 added to CTS solution containing $AgNO_3$ (blue), absent NaBH4 reduction. XRD patterns recorded AgNPs peak at 38.0°, 41.0°, 64.5° and 77.2° (b). This was observed to retain AgNPs in CTS/AgNPs composite (blue), as compared to CTS composite (red).

the silver nitrate were bound to the amine groups of the CTS molecule by chelate bonds (Hang, Tae, & Park, 2010; López-Carballo et al., 2013; Reicha et al., 2012). Consequently, both CTS and silver nitrate were well mixed due to these coordination interactions (Muzzarelli, 2011; Ravi-Kumar, 2000). In the second step, sodium borohydride, an excellent chemical reduction agent, was added to the CTS solution containing silver nitrate. Upon this addition, the solution color changed from pale yellow into dark brown, immediately. This result indicates that the AgNPs were quickly synthesized in the CTS solution (Reicha et al., 2012). This synthesized solution becomes the CTS/AgNPs composite after recrystallization purification (Fig. 1). As shown in (Fig. 2a), the presence of AgNPs in CTS/AgNPs solution was examined by TEM on a dried CTS/AgNPs sample solution on a copper-grid. The TEM image demonstrates that AgNPs were well dispersed in the CTS/AgNPs solution. It also shows that the particles are evenly formed in a spherical shape. The size of the AgNPs from 100 specimens was measured to obtain an average diameter. Sizes between 10 nm and 11 nm size of AgNPs were observed to be the most common and the average diameter of AgNPs was found to be 10 ± 2 nm in the histogram (Fig. 2b) (Krutyakov, Kudrinskiy, Olenin, & Lisichkin, 2008). This result is similar to previous study where silver nitrate interacts with CTS and is subsequently reduced using sodium borohydride (Chen, Zhang, Cao, & Huang, 2013; Shameli et al., 2011). This outcome was also clearly proven via UV–vis absorption spectra peak. The plasmon absorption band was observed in the range of 325–475 nm (Fig. 3a). A narrowed and sharpened wavelength band was also detected at 408 nm which indicates the formation of small-diameter AgNPs in CTS solution (Twu et al., 2008; El-Rafie et al., 2011). This characteristically distinct peak indicates an intense plasmon excitation of AgNPs (El-Rafie et al., 2011; Vimala et al., 2010).

3.2. Characterization of the synthesized CTS/AgNPs composite (XRD, TGA)

After recrystallization, CTS/AgNPs solution became the CTS/AgNPs composite for the use as ELSP material. Freeze-dried CTS/AgNPs composites were characterized by XRD in order to confirm the crystal structure of CTS and AgNPs in the CTS/AgNPs composite (Fig. 3b). The pure CTS and CTS/AgNPs composites were shown to both have a strong peak at 20°, which indicates CTS crystallinity due to the major component chains of CTS. Whereas CTS/AgNPs showed four different peaks as compared to the CTS composite. CTS/AgNPs showed peaks at 38.0°, 44.3°, 64.5° and 77.2° which indicates to (1 1 1), (2 0 0), (2 2 0) and (3 1 1) planes of the face centered cubic structure of AgNPs, respectively (López-Carballo et al., 2013; Shameli et al., 2011). This result found that AgNPs were well dispersed and encapsulated in the CTS/AgNPs composite (JCPDS File No. 04-0783). In order to evaluate the mass content of AgNPs in the CTS/AgNPs, TGA characterization was examined. As shown in Fig. 4, all samples displayed three distinct weight loss regions in 25–800 °C range. The first weight loss region was due to drying of water molecules in the composite substrates at 36 °C, and the second weight loss was due to degradation of the polymer molecules at 239 °C. The third weight loss was different as the CTS composite degraded at 573 °C, whereas the CTS/AgNPs composite degraded at 513 °C. This different maximum decomposition was influenced by AgNPs residue. The mass of the CTS/AgNPs composite at 600–800 °C showed that this residue of AgNPs without any polymer could remain intact at high temperatures. This result also corresponded with previous studies (Ali, Rajendran, & Joshi, 2011; Varaprasad et al., 2011). For these reasons, we demonstrated that the AgNPs was not only well bound to the CTS, but also successful loaded at around 4 wt.% in the CTS/AgNPs composite.

3.3. Viscometry characterization of CTS/AgNPs solutions (viscometer)

As shown in Table 1, the viscosity measurements of CTS and CTS/AgNPs solutions by viscometer were 424, 252, 281, 364 and 416 mPa s for AgNPs contents of 0, 4, 2, 1.3 and 0.7 wt.%,

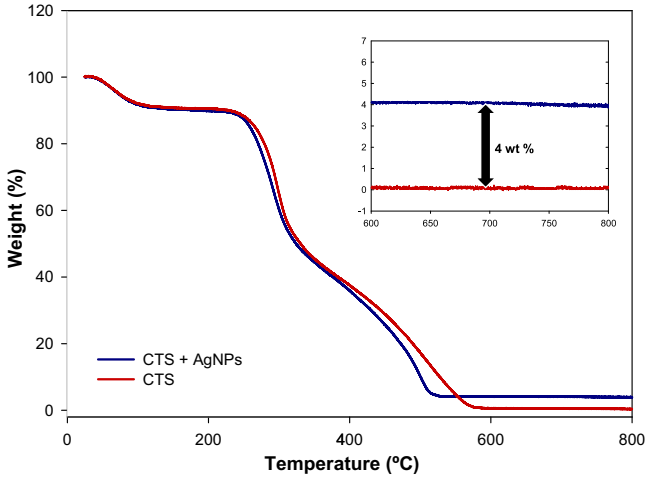

Fig. 4. Thermogram curves of CTS/AgNPs composite (blue), and CTS composite (red). As shown in the small diagram, the presence of 4 wt.% AgNPs in CTS/AgNPs composite were confirmed with maximum decompositions at 600–800 °C.

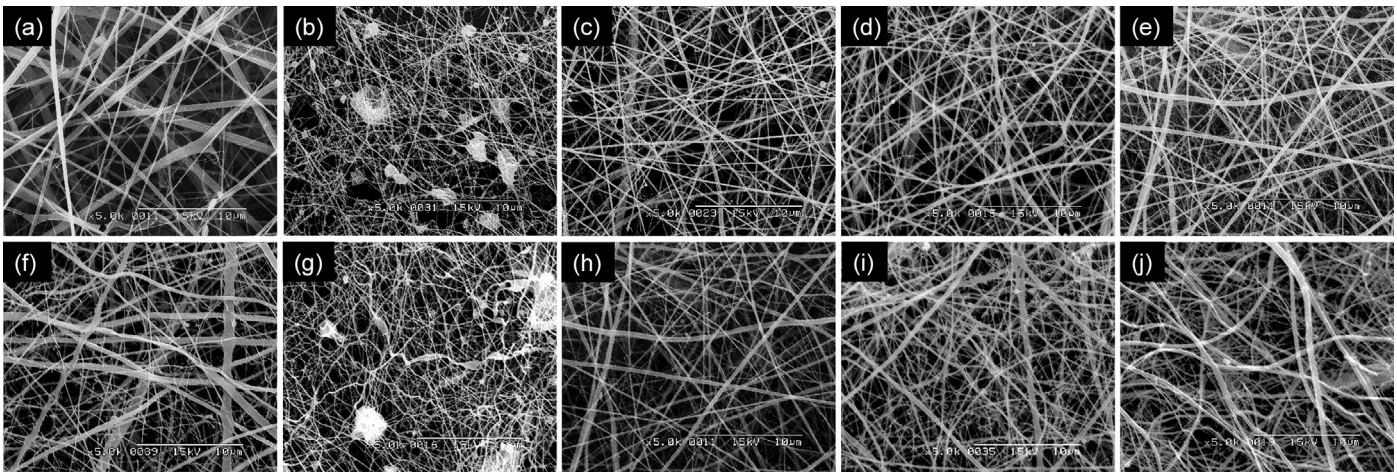

Fig. 5. SEM images of CTS and CTS/AgNPs nanofibers fabricated by electrospinning. Pre-neutralization (a–e) and after-neutralization (f–j). CTS nanofiber (a), CTS/AgNPs nanofiber (b), CTS:CTS/AgNPs = 50:50 (c), CTS:CTS/AgNPs = 67:33 (d), CTS:CTS/AgNPs = 83:17 (e).

respectively. The viscosity of ELSP solutions were observed to decrease upon an increase in the content of the CTS/AgNPs composite. The viscosity measurements are well correlated to the solution surface tension. The relationship between viscosity and surface tension is well known for an inverse proportion curve (Deitzel, Kleinmeyer, Harris. & Beck Tan, 2001). Surface tension might be increased due to a decrease in the viscosity. Either solution surface tension or viscosity plays an important role in determining the diameter of ELSP fibers. The various ratios of fabricated fibers showed differences in diameter and bead formation. The AgNPs with a content of 4 wt.% solution had the lowest viscosity, meaning the highest surface tension as compared to other specimen properties. As shown in Fig. 5b, the AgNPs with a content of 4 wt.% were observed to form beads which could be attributable to high surface tension and low viscosity of the solution due to increased silver content (Khalil, Fouad, Elsarnagawy, & Almajhdi, 2013). The solution viscosity has an impact on fiber morphology. The high viscosity solutions have longer stress behavior or long relaxation time, which could avoid the fracturing of the released jets during ELSP (Li, He, Zheng, & Han, 2006). On the other hand, the low viscosity solutions have a undesirable influence towards fabricating the fiber during ELSP. This is because the spray jet breaks up into small beads resulting in a mixture of fiber and discrete beads of material (Ramakrishna, 2005).

3.4. Morphological characterization of CTS/AgNPs nanofibers (SEM, TEM)

Fig. 5 shows SEM micrographs of the varying nanofibers respectively. We obtained CTS and CTS/AgNPs nanofibers via the ELSP technique. We chose this method of mixing the composite because quantitative measurements of AgNPs were difficult and it was too small to accurately weigh. As shown in Fig. 5a and c–e, homogeneous nanofibrous structures were observed with uniform morphology. On the other hand, Fig. 5b shows that AgNPs with a content of 4 wt.% in the nanofiber had entwined beads and a tangled surface morphology. Handling of this sheet after neutralization is difficult and may hinder its performance as a wound dressing (Fig. S1). For this reason the AgNPs/CTS with a 4 wt.% AgNPs were excluded from the antibacterial activity test. As shown in Fig. 5 and Table 1, the average diameters of CTS and CTS/AgNPs nanofibers were 460 ± 80 nm, 126 ± 28 nm, 238 ± 46 nm, 337 ± 49 nm and 349 ± 56 nm for AgNPs contents of 0, 4, 2, 1.3 and 0.7 wt.%, respectively. The diameters of these nanofibers were observed to decrease upon an increase in the content of the AgNPs (Sheikh et al., 2008). Due to the presence of AgNPs in the CTS/AgNPs solution there was an increased electrical charge and conductivity of this solution which resulted in a thinner diameter of the fibers (Saquing, Manasco, & Khan, 2009; Son, Youk, Lee, & Park, 2004). The micrographs of Fig. 5f–j were obtained after neutralization of CTS and CTS/AgNPs nanofibers. Each of these fibers was observed to swell slightly as compared to the non-neutralization nanofibers. However, these neutralized fibers were not observed to have any significant difference in fiber diameter and morphology as compared to the fibers shown in Fig. 5a–e. The TEM images (Fig. 6) clearly indicate whether the nanofibers did or did not contain AgNPs. Pure CTS nanofibers shown in Fig. 6a did not indicate the presence of any particles but CTS/AgNPs loaded nanofibers shown in Fig. 6b–e were observed to have AgNPs well distributed in these fibers. Additionally, the quantity of AgNPs was observed to reduce from Fig. 6b to e indicating a gradually decreasing AgNPs content. Likewise, with SEM images, the neutralized nanofibers of the TEM images (Fig. 6f–j) did not differ in their morphology in respect to the non-neutralized images shown in Fig. 6a–e.

3.5. Zone of inhibition testing of antibacterial efficacy. P. aeruginosa and MRSA

The bacterial inhibition test of the CTS and the CTS/AgNPs nanofibers against *P. aeruginosa* and MRSA were performed. To confirm whether CTS/AgNPs nanofibers have an effective antibacterial

Table 1
CTS and various blending ratios of CTS/AgNPs nanofibers fabricated by electrospinning.

	CTS:CTS/AgNPs	Content AgNPs (wt %)	Diameter (nm)	Viscosity (mPa s)
(a)	100:0	0	460 ± 80	424
(b)	0:100	4	126 ± 28	252
(c)	50:50	2	238 ± 46	281
(d)	67:33	1.3	337 ± 49	364
(e)	83:17	0.7	349 ± 56	416

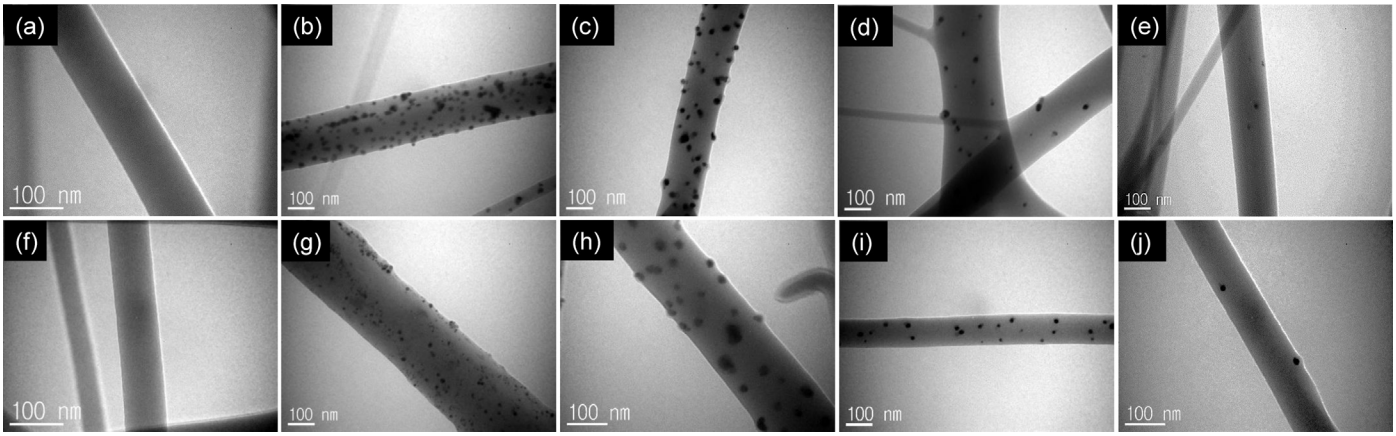

Fig. 6. TEM images of CTS and CTS/AgNPs nanofibers fabricated by electrospinning. Pre-neutralization (a–e) and after-neutralization (f–j). CTS nanofiber (a), CTS/AgNPs nanofiber (b), CTS:CTS/AgNPs = 50:50 (c), CTS:CTS/AgNPs = 67:33 (d), CTS:CTS/AgNPs = 83:17 (e).

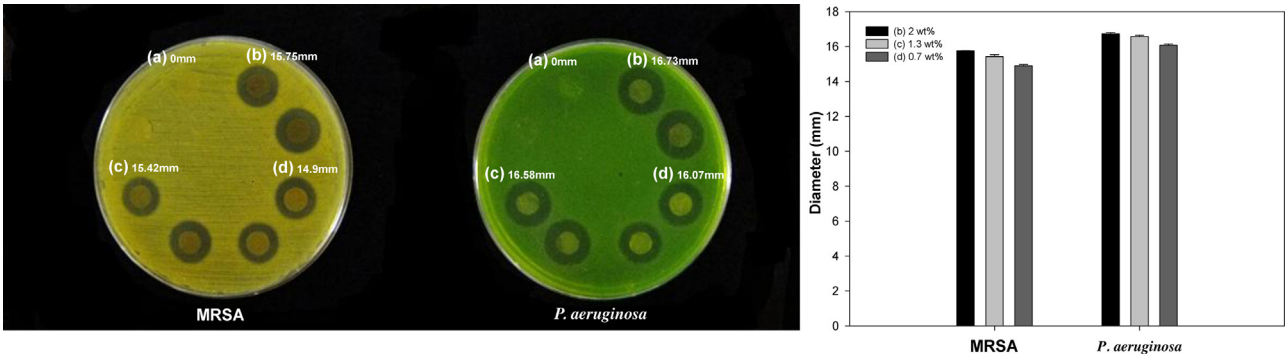

Fig. 7. Zone of inhibition antibacterial testing against MRSA (dark yellow) and *P. aeruginosa* (green), each sample represents after-neutralization (a–d) CTS nanofibers. (a) CTS:CTS/AgNPs = 50:50, (b) CTS:CTS/AgNPs = 67:33, (c) CTS:CTS/AgNPs = 83:17 (d). Schematic diagram is shown that measured dimension of inhibited bacteria due to contained AgNPs effect.

activity, pure CTS nanofiber was used as blank control and various ratios of CTS/AgNPs nanofibers were used as comparative samples. As shown in Fig. 7, both *P. aeruginosa* (green plate) and MRSA (dark yellow plate) clearly showed a zone of inhibited growth of the bacteria around the CTS/AgNPs nanofibers. The degree of the diameter for each sample is shown in the schematic diagram. As can be seen, pure CTS nanofiber displayed no inhibition of bacteria. On the contrary, CTS/AgNPs nanofibers were shown to inhibit the growth of bacteria with slightly higher effectiveness against *P. aeruginosa* (green plate) as compared to MRSA (dark yellow plate). Here we distinctly demonstrated that bacterial growth was inhibited depending upon the presence of AgNPs in the fiber. The antibacterial tests of CTS and CTS/AgNPs nanofibers against *P. aeruginosa* also showed that the zones of inhibition for the CTS/AgNPs = 100:0, 50:50, 67:33, 83:17 (AgNPs contents = 0, 2, 1.3, 0.7 wt.%) were 0 mm, 16.73 mm, 16.58 mm, 16.07 mm, respectively. The zones of inhibition for MRSA was shown to be for CTS/AgNPs = 100:0, 50:50, 67:33, 83:17 (AgNPs contents = 0, 2, 1.3, 0.7 wt.%) as 0 mm, 15.75 mm, 15.42 mm, 14.9 mm, respectively. This result indicates that as the quantity of AgNPs increased in these fibers, the antibacterial effects were enhanced. This indicates that the AgNPs content could be adjusted to control the antibacterial effect. Bacteria are affected by AgNPs as these particles are lethal to bacteria. First, AgNPs adhere to a negatively charged of cell membrane surface. This phenomenon leads to a loss of permeability and influences the respiration chain. Secondly, the AgNPs penetrate into the cell body which leads to damage due to interaction with sulfur and phosphorus found in biological components such as DNA. Finally, AgNPs induce cell-lysis, cell leakage, in the end cell death (Fouda et al., 2013; Lago et al., 2011; Rai et al., 2009). It has also been recently reported (Xiu, Zhang, Puppala, Colvin, & Alvarez, 2012) that silver ions released from AgNPs can have an antifungal function. In this case the CTS/AgNPs nanofibers act as a delivery vehicle for the silver ions. As seen in all of these results, the CTS/AgNPs nanofibers have a good potential for use as a biocompatible and antimicrobial wound dressing.

4. Conclusion

In summary, the varying ratios of homogeneous CTS/AgNPs nanofibers at blends of 100:0, 0:100, 50:50, 67:33, 83:17 (AgNPs contents = 0, 4, 2, 1.3, and 0.7 wt.%) were successfully fabricated by ELSP method and neutralized. Our results indicate that approximately 10 nm sized AgNPs were well dispersed in the CTS/AgNPs nanofiber. AgNPs were synthesized directly by chemical reduction within the CTS solution and this synthesis was confirmed by physical analysis. The presences of AgNPs were shown to vary by the content in each of the blended fibers. Also, the CTS/AgNPs nanofibers displayed a surprising phenomenon in that the diameters were gradually decreased as the content of AgNPs were increased. This may be due to the decrease of viscosity of the CTS/AgNPs ELSP solution upon an increase in the content of the CTS/AgNPs composite. The content of AgNPs in the CTS/AgNPs solution was found to be strongly affecting the electrospun nanofibers diameters and to generate fiber beads due to enhancement of surface tension of ELSP solution. In antibacterial testing, the pure CTS nanofibers were observed to not substantially inhibit bacterial growth. But CTS/AgNPs nanofibers displayed a high degree of effectiveness against *P. aeruginosa* and MRSA. Also, the CTS/AgNPs

nanofibers were slightly more effective against *P. aeruginosa* (green plate) as compared to MRSA (dark yellow plate). Additionally as the quantity of AgNPs was increased in the fibers, its antibacterial properties were enhanced against both microorganisms. Thus, we proved that CTS/AgNPs nanofibers have a very strong antimicrobial activity. As a result, these CTS/AgNPs nanofibers can be used as potent antibacterial wound dressing materials in the biomedical field.

Acknowledgments

This work was supported by the National Research Foundation of Korea (NRF) grant funded by the Ministry of Education, Science and Technology (Nos. NRF-2012R1A5A2051388, NRF-2010-0019346) and the Technology Innovation Program of Ministry of Knowledge Economy (MKE) (No. 10035291).

Appendix A. Supplementary data

Supplementary data associated with this article can be found, in the online version, at http://dx.doi.org/10.1016/j.carbpol.2014.04.026.

References

Ali, S. W., Rajendran, S., & Joshi, M. (2011). Synthesis and characterization of chitosan and silver loaded chitosan nanoparticles for bioactive polyester. *Carbohydrate Polymers*, *83*, 438–446.

Atiyeh, B. S., Costagliola, M., Hayek, S. N., & Dibo, S. A. (2007). Effect of silver on burn wound infection control and healing: review of the literature. *Burns*, *33*(2), 139–148.

Bhardwaj, N., & Kundu, S. C. (2010). Electrospinning: A fascinating fiber fabrication technique. *Biotechnology Advances*, *28*, 325–347.

Bhattarai, B. N., Li, Z., Gunn, J., Leung, M., Cooper, A., Edmondson, D., Veiseh, O., Chen, M. H., Zhang, Y., Ellenbogen, R. G., & Zhang, M. (2009). Natural-synthetic polyblend nanofibers for biomedical applications. *Advanced Materials*, *21*, 2792–2797.

Burger, C., Hsiao, B. S., & Chu, B. (2006). Nanofibrous and their applications. *Annual Review of Materials Research*, *36*, 333–368.

Cao, X. L., Cheng, C., Ma, Y. L., & Zhao, C. S. (2010). Preparation of silver nanoparticles with antimicrobial activities and the researches of their biocompatibilities. *Journal of Materials Science: Materials in Medicine*, *21*, 2861–2868.

Chaloupka, K., Malam, Y., & Seifalian, A. M. (2010). Nanosilver as a new generation of nanoproduct in biomedical applications. *Trends in Biotechnology*, *28*(11), 580–588.

Chen, Z., Zhang, X., Cao, H., & Huang, Y. (2013). Chitosan-capped silver nanoparticles as a highly selective colorimetric probe for visual detection of aromatic ortho-trihydroxy phenols. *Analyst*, *138*, 2343–2349.

Deitzel, J., Kleinmeyer, J., Harris, D. E. A., & Beck Tan, N. (2001). The effect of processing variables on the morphology of electrospun nanofibers and textiles. *Polymer*, *42*(1), 261–272.

El-Rafie, M. H., El-Naggar., M. E., Ramadan, M. A., Fouda, M. M. G., Al-Deyab, S. S., & Hebeish, A. (2011). Environmental synthesis of silver nanoparticles using hydroxypropyl starch and their characterization. *Carbohydrate Polymers*, *86*, 630–635.

Elsabee, M. Z., Naguib, H. F., & Morsi, R. E. (2012). Chitosan based nanofibers, review. *Materials Science and Engineering: C*, *32*(7), 1711–1726.

Fouda, M. M. G., El-Aassar, M. R., & Al-Deyab, S. S. (2013). Antimicrobial activity of carboxymethyl chitosan/polyethylene oxide nanofibers embedded silver nanoparticles. *Carbohydrate Polymers*, *92*, 1012–1017.

Greiner, A., & Wendorff, J. H. (2007). Electrospinning: A fascinating method for the preparation of ultrathin fibers. *Nanotechnology*, *46*, 5670–5703.

Guibal, E. (2005). Heterogeneous catalysis on chitosan-based materials: A review. *Progress in Polymer Science*, *30*, 71–109.

Hang, A. T., Tae, B., & Park, J. S. (2010). Non-woven mats of poly(vinyl alcohol)/chitosan blends containing silver nanoparticles: Fabrication and characterization. *Carbohydrate Polymers*, *82*, 472–479.

Jayakumar, R., Prabaharan, M., Nair, S. V., & Tamura, H. (2010). Novel chitin and chitosan nanofibers in biomedical applications. *Biotechnology Advances*, *28*, 142–150.

Jin, W. J., Lee, H. K., Jeong, E. H., Park, W. H., & Youk, J. H. (2005). Preparation of polymer nanofibers containing silver nanoparticles by using poly(N-vinylpyrrolidone). *Macromolecular Rapid Communications*, *26*, 1903–1907.

Jin, G., Prabhakaran, M. P., Kai Dan Annamalai, S. K., Arunachalam, K. D., & Ramakrishna, S. (2013). Tissue engineered plant extracts as nanofibrous wound dressing. *Biomaterials*, *34*, 724–734.

Khalil, K. A., Fouad, H., Elsarnagawy, T., & Almajhdi, F. N. (2013). Preparation and characterization of electrospun PLGA/silver composite nanofibers for biomedical applications. *International Journal of Electrochemical Science*, *8*, 3483–3493.

Khor, E., & Lim, L. Y. (2003). Implantable applications of chitin and chitosan. *Biomaterials*, *24*, 2339–2349.

Kong, H., & Jang, J. (2008a). Antibacterial properties of novel poly(methyl methacrylate) nanofiber containing silver nanoparticles. *Langmuir*, *24*, 2051–2056.

Kong, H., & Jang, J. (2008b). Synthesis and antimicrobial properties of novel silver/polyrhodanine nanofibers. *Biomacromolecules*, *9*, 2677–2681.

Krutyakov, Yu. A., Kudrinskiy, A. A., Olenin, A., & Yu Lisichkin, G. V. (2008). Synthesis and properties of silver nanoparticles: Advances and prospects. *Russian Chemical Reviews*, *77*, 233–257.

Lago, V. D., Oliveira, L. F. D., Gonçalves, K. D. A., Kobarg, J., & Cardoso, M. B. (2011). Size-selective silver nanoparticles: Future of biomedical devices with enhanced bactericidal properties. *Journal of Materials Chemistry*, *21*, 12267–12273.

Lee, K. Y., Jeong, L., Kang, Y. O., Lee, S. J., & Park, W. H. (2009). Electrospinning of polysaccharides for regenerative medicine. *Advanced Drug Delivery Reviews*, *61*, 1020–1032.

Li, J., He, A., Zheng, J., & Han, C. C. (2006). Gelatin and gelatin-hyaluronic acid nanofibrous membranes produced by electrospinning of their aqueous solutions. *Biomacromolecules*, *7*(7), 2243–2247.

López-Carballo, G., Higueras, L., Gavara, R., & Hernández-Muñoz, P. (2013). Silver ions release from antibacterial chitosan films containing in situ generated silver nanoparticles. *Journal of Agricultural and Food Chemistry*, *61*, 260–267.

Mahoney, C., Mccullough, M., Sankar, J., & Bhattarai, N. (2012). Nanofibrous structure of chitosan for biomedical applications. *Journal of Nanomedicine & Biotherapeutic Discovery*, *2*, 1–9.

Morones, J. R., Elechiguerra, J. L., Camacho, A., Holt, K., Kouri, J. B., Ramírez, J. T., & Yacaman, M. J. (2005). The bactericidal effect of silver nanoparticles. *Nanotechnology*, *16*, 2346–2353.

Muzzarelli, R. A. A. (2011). Potential of chitin/chitosan-bearing materials for uranium recovery: An interdisciplinary review. *Carbohydrate Polymers*, *84*, 54–63.

Muzzarelli, R. A. A., & Muzzaralli, C. (2005). Chitosan chemistry: Relevance to the biomedical sciences. *Advanced Polymer Science*, *186*, 151–209.

Pal, S., Tak, Y. K., & Song, J. M. (2007). Does the antibacterial activity of silver nanoparticles depend on the shape of the nanoparticle? A study of the gram-negative bacterium Escherichia coli. *Applied and Environmental Microbiology*, *73*(6), 1712–1720.

Pham, Q. P., Sharma, U., & Mikos, A. G. (2006). Electrospinning of polymeric nanofibers for tissue engineering applications: A review. *Tissue Engineering*, *12*(5), 1197–1211.

Rai, M., Yadav, A., & Gade, A. (2009). Silver nanoparticles as a new generation of antimicrobials. *Biotechnology Advances*, *27*, 76–83.

Ramakrishna, S. (2005). *An introduction to electrospinning and nanofibers*. World Scientific.

Ravi-Kumar, M. N. V. (2000). A review of chitin and chitosan applications. *Reactive and Functional Polymers*, *46*, 1–27.

Reicha, F. M., Sarhan, A., Hamid, M. I. A., & Sherbiny, I. M. E. (2012). Preparation of silver nanoparticles in the presence of chitosan by electrochemical method. *Carbohydrates Polymers*, *89*, 236–244.

Rujitanaroj, P. O., Pimpha, N., & Supaphol, P. (2008). Wound-dressing materials with antibacterial activity from electrospun gelatin fiber mats containing silver nanoparticles. *Polymer*, *49*, 4723–4732.

Saquing, C. D., Manasco, J. L., & Khan, S. A. (2009). Electrospun nanoparticle-nanofiber composites via a one-step synthesis. *Small*, *8*, 944–951.

Sencadas, V., Correia, D., Areias, A., Botelho, G., Fonseca, A., Neves, I., Gomez Ribelles, J., & Lanceros Mendez, S. (2012). Determination of the parameters affecting electrospun chitosan fiber size distribution and morphology. *Carbohydrate Polymers*, *87*(2), 1295–1301.

Shameli, K., Ahmad, M. B., Zargar, M., Yunus, W. M., Ibrahim, N. A., Shabanzadeh, P., & Moghaddam, M. G. (2011). Synthesis and characterization of silver/montmorillonite/chitosan bionanocomposites by chemical reduction method and their antibacterial activity. *International Journal of Nanomedicine*, *6*, 271–284.

Sheikh, F. A., Barakat, N. A. M., Kanjwal, M. A., Jeon, S. H., Kang, H. S., & Kim, H. Y. (2008). Self synthesize of silver nanoparticles in/on polyurethane nanofibers: Nano-biotechnological approach. *Journal of Applied Polymer Science*, *6*, 3189–3198.

Son, W. K., Youk, J. H., Lee, T. S., & Park, W. H. (2004). The effects of solution properties and polyelectrolyte on electrospinning of ultrafine poly(ethylene oxide) fibers. *Polymer*, *45*, 2959–2966.

Song, J., Kang, H., Lee, C., Hwang, S. H., & Jang, J. (2012). Aqueous synthesis of silver nanoparticle embedded cationic polymer nanofibers and their antibacterial activity. *ACS Applied Materials & Interfaces*, *4*, 460–465.

Storm-Versloot, M. N., Vos, C. G., Ubbink, D. T., & Vermeulen, H. (2010). Topical silver for preventing wound infection. *Cochrane Database Syst Rev*, 3.

Twu, Y. K., Chen, Y. W., & Shih, C. M. (2008). Preparation of silver nanoparticles using chitosan suspensions. *Powder Technology*, *185*, 251–257.

Varaprasad, K., Vimala, K., Ravindra, S., Narayana, R. N., Venkata, S. R. G., & Mohana, R. K. (2011). Fabrication of silver nanocomposite films impregnated with curcumin for superior antibacterial applications. *Journal of Materials Science: Materials in Medicine*, *22*, 1863–1872.

Vimala, K., Mohan, Y. M., Sivudu, K. S., Varaprasad, K., Ravindra, S., Reddy, N. N., Padma, Y., Sreedhar, B., & MohanaRaju, K. (2010). Fabrication of porous

chitosan films impregnated with silver nanoparticles: a facile approach for superior antibacterial application. *Colloids and Surfaces B: Biointerfaces*, *76*, 248–258.
Xie, J., Li, X., & Xia, Y. (2008). Putting electrospun nanofibers to work for biomedical research. *Macromolecular Rapid Communications*, *29*, 1775–1792.
Xing, Z. C., Chae, W. P., Baek, J. Y., Choi, M. J., Jung, Y., & Kang, I. K. (2010). In vitro assessment of antibacterial activity and cytocompatibility of silver-containing PHBV nanofibrous scaffolds for tissue engineering. *Biomacromolecules*, *11*, 1248–1253.
Xiu, Z. M., Zhang, Q. B., Puppala, H. L., Colvin, V. L., & Alvarez, P. J. (2012). Negligible particle-specific antibacterial activity of silver nanoparticles. *Nano Letters*, *12*, 4271–4275.
Yoshimoto, H., Shin, Y. M., Terai, H., & Vacanti, J. P. (2003). A biodegradable nanofiber scaffold by electrospinning and its potential for bone tissue engineering. *Biomaterials*, *24*, 2077–2082.
Zhuang, X., Cheng, B., Kang, W., & Xu, X. (2010). Electrospun chitosan/gelatin nanofibers containing silver nanoparticles. *Carbohydrate Polymers*, *82*, 524–527.